Author's Accepted Manuscript

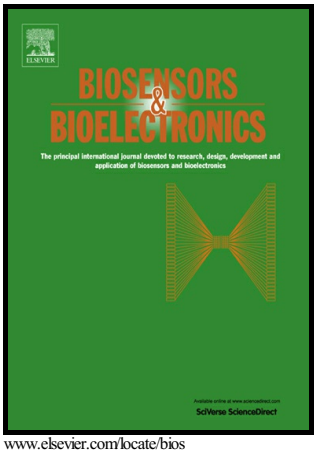

www.elsevier.com/locate/bios

A Simple and Efficient Design to Improve the Detection of Biotin-Streptavidin Interaction with Plasmonic Nanobiosensors

Monica Focsan, Andreea Campu, Ana-Maria Craciun, Monica Potara, Cosmin Leordean, Dana Maniu, Simion Astilean

PII: S0956-5663(16)30684-4
DOI: http://dx.doi.org/10.1016/j.bios.2016.07.054
Reference: BIOS8935

To appear in: *Biosensors and Bioelectronic*

Received date: 26 April 2016
Revised date: 29 June 2016
Accepted date: 16 July 2016

Cite this article as: Monica Focsan, Andreea Campu, Ana-Maria Craciun Monica Potara, Cosmin Leordean, Dana Maniu and Simion Astilean, A Simple and Efficient Design to Improve the Detection of Biotin-Streptavidin Interactio with Plasmonic Nanobiosensors, *Biosensors and Bioelectronic* http://dx.doi.org/10.1016/j.bios.2016.07.054

This is a PDF file of an unedited manuscript that has been accepted fo publication. As a service to our customers we are providing this early version o the manuscript. The manuscript will undergo copyediting, typesetting, an review of the resulting galley proof before it is published in its final citable form Please note that during the production process errors may be discovered whic could affect the content, and all legal disclaimers that apply to the journal pertain

ACCEPTED MANUSCRIPT

A Simple and Efficient Design to Improve the Detection of Biotin-Streptavidin Interaction with Plasmonic Nanobiosensors

Monica Focsan[a], Andreea Campu[a], Ana-Maria Craciun[a], Monica Potara[a], Cosmin Leordean[a]
Dana Maniu[a,b], Simion Astilean[a,b]*

[a] Interdisciplinary Research Institute on Bio-Nano-Sciences, Babes-Bolyai University, Treboniu Laurean Str. 42, Cluj-Napoca 400271, Romania

[b] Biomolecular Physics Department, Faculty of Physics, Babes-Bolyai University, M Kogalniceanu Str. 1, Cluj-Napoca 400084, Romania

*Corresponding author: Tel: +40 264 405300/5188; Fax: +40 264 591906; e-mail address: simion.astilean@phys.ubbcluj.ro

In this manuscript we propose a simple and efficient strategy to improve the sensitivity of localized surface plasmon resonance (LSPR) shift-based biosensors using biotin-streptavidin recognition interaction as a proof-of-concept. Specifically, biotin molecules are immobilized on a low-cost plasmonic LSPR biosensor based on annealed self-assembled spherical gold nanoparticles (AuNSs) and successively incubated with increasing concentrations of streptavidin, achieving a limit of detection (LOD) of 5 nM. Interestingly, when the detection is performed by the same biotin-functionalized plasmonic AuNSs substrate but against streptavidin previously conjugated to gold nanorods, the LSPR shift is 26-fold enhanced. Moreover, we confirm these results through numerical simulations and demonstrate that the proposed sensing architecture can operate as transducer not only to confirm the adsorption of bioanalyte but also to provide the chemical identity of the capture and targeted molecules from their vibrational Raman fingerprints. Therefore, we are confident that the development of such plasmonic biosensors that use metallic labels for improving the sensitivity of detection could become highly promising for future point-of-care diagnostic assays, pushing sensitivity towards single-molecule detection limit.

Keywords: LSPR biosensors; SERS platform; improved detection

Accepted manuscript

ACCEPTED MANUSCRIPT

1. Introduction

New strategies for the development of sensing devices that can detect analyte species without labeling, *i.e.* label-free detection, are of significant interest today in biosensor research (Abbas et al., 2013; Guo et al., 2015). Optical sensors based on plasmonic transducers are fast becoming the method of choice in non-labeling analysis of biomolecular interaction. The conventional plasmonic sensors based on the excitation of extended surface plasmons resonance (SPR) on planar gold surface (Kretschmann configuration) serve currently as reference standard for optically addressed sensors (Rich and Myszka, 2010). Depending on the protocol used for the SPR detection, the amplification of the signal can be improved, obtaining biologically relevant limit of the detection. Just for example, vascular endothelial growth factor (VEGF) has been detected by SPR at biologically levels of 45 pM (Thanh and Rosenzweig, 2002). Alternative techniques to SPR-based detection could be Fourier transform infrared/ attenuated total intern reflection (FTIR- ATR) -based biodetection, bringing new spectroscopic information, especially information related to the conformation of biomolecules/proteins (Liley et al., 1997; Voue et al., 2007). Thus, these techniques are promising for the detection of biomarkers, but real problems still remains their validation in stable, portable and miniaturize devices, limiting thus their further integration into point-of-care applications.

Recently, there has been an increasing interest in the development of localized SPR (LSPR) sensors based on individual metallic nanoparticles (NPs) as low-cost alternative to conventional SPR sensors, being identified as the next generation of optical label-free biosensors. The resonance wavelength of LSPR is determined by NPs's size, shape, interparticle spacing and local dielectric environment (Zhao et al., 2006). Specifically, the LSPR phenomena can detect shifts of the resonance wavelength in response to changes of the refractive index of the medium surrounding the plasmonic NPs thus providing the basis of LSPR biosensors (Anker et al., 2008). In a typical LSPR biosensor configuration, when biomolecules start to bind to the surface of NPs by chemo- or physic-sorption, the surface polarization and -implicitly- the dielectric function of local environment changes. The modification of dielectric function transduces the biomolecular binding event by tuning the resonance peak and the readout of LSPR response is quantified into a resonant wavelength red-shift and/or maximum optical density changes (Zhao et al., 2006). These undoubtedly

Accepted manuscript

ACCEPTED MANUSCRIPT

advantages allow this technique to be successfully implemented for a label-free highly sensitive molecular detection (Hall et al., 2011a; Svedendahl et al., 2009). Due to nanoscale localized sensing and easily integration with microfluidic devices for portable optofluidic sensing, LSPR sensors promise to be effective in a range of biomedical applications (Al Balushi et al., 2013; Ament et al., 2012; Geng et al., 2014; Mayer and Hafner, 2011).

Although LSPR sensing mechanism is rather simple, LSPR sensors have a reduced sensitivity (< 1000 nm/RIU) and lower figure of merit (<100 RIU^{-1}) when compared with standard plasmonic biosensors that utilize extended SPR, having a spectral sensitivity well above 10^4 nm/RIU, as it was previously reported (Mayer and Hafner, 2011; White and Fan, 2008). The implementation of reliable LSPR biosensors of high sensitivity is a difficult task which requires not only the production of NPs of well-controlled size and shape but also the specific functionalization of the NPs' surface to allow the capture of the target-specific biomolecules from simulated solution or real biological fluid. Furthermore, in the field of biomedical diagnostic is an essential need to develop simple, affordable, robust biosensors to allow both rapid and portable determination of various relevant analytes, where regular assays for protein analytes, such as enzyme-linked immunosorbent assay (ELISA) for example, cannot be performed. In this context, one typical strategy to enhance the LSPR sensitivity is to use NPs of high aspect ratio (ellipsoidal NPs, nanorods, bipyramids) as plasmonic transducers which perform better than spherical ones.

Although diverse detection schemes have been reported in literature (Guo and Kim, 2012; Szunerits and Boukherroub, 2012), there has been limited progress in improving the sensitivity of LSPR shift-based biosensors. In common LSPR experiments the recognition element is attached to the surface of isolated plasmonic NP and the detection is inferred from LSPR shift as result of chemical capture of the bioanalyte from solution. The originality of our nanosensors lies in its sandwich plasmonic architecture which we build to localize the molecular recognition interaction not at the surface of unique NP but in between or in close vicinity of electromagnetically coupled several NPs. As proof-of-concept for enhanced sensitivity of our plasmonic biosensors we use the biotin-streptavidin recognition interaction. Specifically, the capture biotin molecules are immobilized on inexpensive annealed spherical gold NPs (AuNSs) self-assembled on solid surface and successively incubated with increasing concentrations of streptavidin, achieving a limit of

Accepted manuscript

ACCEPTED MANUSCRIPT

detection (LOD) of 5 nM. Interestingly, when the detection is performed by the same biotin-functionalized plasmonic AuNSs substrate but against streptavidin of same concentration previously conjugated to gold nanorods (AuNRs), the LSPR shift is 26-fold enhanced. Furthermore, by detecting a streptavidin concentration of 2 nM, we prove the ability of this strategy to enhance LSPR shifts for more sensitive detection of low concentrations of analytes. In addition, our sensing architecture can operate as high sensitive transducer in two ways. Firstly, we demonstrate that the spectral profile of LSPR is sensitive to the capture of bioanalyte and, secondly, the enhancement of local electromagnetic field of LSPR leads to Surface Enhanced Raman Scattering (SERS) signal which allows ascertaining the chemical identity of the capture and targeted molecules from their vibrational fingerprints. Our experimental results are supported by numerical simulations performed using Finite-Difference Time-Domain method. The development of such plasmonic biosensors that use metallic labels for sensitivity improvement becomes highly promising for future point-of-care diagnostic assays, pushing sensitivity towards the single-molecule detection limit. More importantly, the proposed biosensor can be easily integrate into portable, low-cost and real-life miniaturized devices for rapid and less invasive bioanalytical measurements.

2. Material and Methods

2.1. Materials

Tetrachloroauric (III) acid ($HAuCl_4$), trisodium citrate ($Na_3C_6H_5O_7 \cdot 2H_2O$), cetyltrimethylammonium bromide (CTAB), ascorbic acid, Bovine Serum Albumin (BSA, 66 kDa), (3-Aminopropyl)triethoxysilane (APTES), (3-Mercaptopropyl)triethoxysilane (MPTES) and (+)-Biotin N-hydroxysuccinimide ester (biotin-NHS) were purchased from Aldrich. Sodium borohydride ($NaBH_4$, 99 %) and silver nitrate ($AgNO_3$) were obtained from Merck. Streptavidin was acquired from Calbiochem. All chemicals were used as received.

2.2. Synthesis of Gold Nanoparticles in solution

Colloidal AuNSs were synthesized according to the Turkevich method by chemical reduction of $HAuCl_4$ with sodium citrate (Turkevich et al., 1951). The as-prepared AuNSs in solution exhibit a plasmonic resonance at 520 nm and an average diameter of 18 ± 2 nm, as previously demonstrated (Suarasan et al.,

ACCEPTED MANUSCRIPT

2013) , parameters which are consistent with hydrodynamic diameter of 23 nm with a standard deviation of ± 2.9 nm and zeta potential of – 41 ± 1.2 mV (ξ-deviation = 3.1) (Fig. S1).

Colloidal AuNRs were synthesized utilizing the seed-mediated growth method (Nikoobakht and El-Sayed, 2003). Gold seeds were firstly prepared by mixing 1.25 mL of 5 mM $HAuCl_4$, 1.25 mL of 0.2 M CTAB and 0.9 mL of freshly prepared ice cold 1 mM $NaBH_4$ solution under continuous stirring, resulting in a brownish yellow solution. The growth solution was obtained by mixing 5 mL of 1 mM $HAuCl_4$ with 5 mL of 0.2 M CTAB and 4 mM $AgNO_3$. 0.07 mL of 0.0788 M ascorbic acid was then added while gently stirring. Ascorbic acid acts as a mild reducing agent and changes the color of growth solution from dark yellow to colorless. Finally, 0.012 mL of seed solution was added into the as-prepared solution in order to start the growth of nanorods. The color of the solution gradually changed in the first 15-20 min before finally stabilizing. The obtained AuNRs were collected twice by centrifugation in order to remove the excess CTAB surfactant and then dispersed in ultrapure water. Based on our previous results, the average length, diameter and aspect ratio of the synthesized AuNRs are 34 nm, 10.5 nm and 3.2, respectively (Canpean et al., 2013).

2.3. Large-scale fabrication of the plasmonic biosensor

First, to improve the reactivity of the glass solid surface and to remove any organic remaining contaminants, the glass substrate was cleaned with chromic acid solution, washed thoroughly with ultrapure water and further treated in ozone cleaner (PSDP-UVT - Benchtop UV Cleaner) for 20 min. Second, the as-cleaned glass substrate was silanized through immersion in a 1% (v/v) MPTES methanol solution for 1 h. In order to remove any loosely adsorbed MPTES molecules, the substrate was rinsed with methanol and ultrapure water several times. The as-functionalized substrate was subsequently immersed into a solution of pre-synthesized AuNSs for another 3 h to allow the assembling of the NPs. The obtained AuNSs substrate was dried and transferred into a high-temperature oven (Barnstead Thermolyne Type 47900 Furnace) to conduct thermal annealing at 500°C for 90 min. The annealed AuNSs substrate was left to cool at room temperature and subsequently used as platform in the construction of our sensitive LSPR immunosensors.

Accepted manuscript

2.4 Biosensing protocol

The proposed biosensing protocol using the annealed AuNSs substrate is schematic illustrated in Scheme 1.

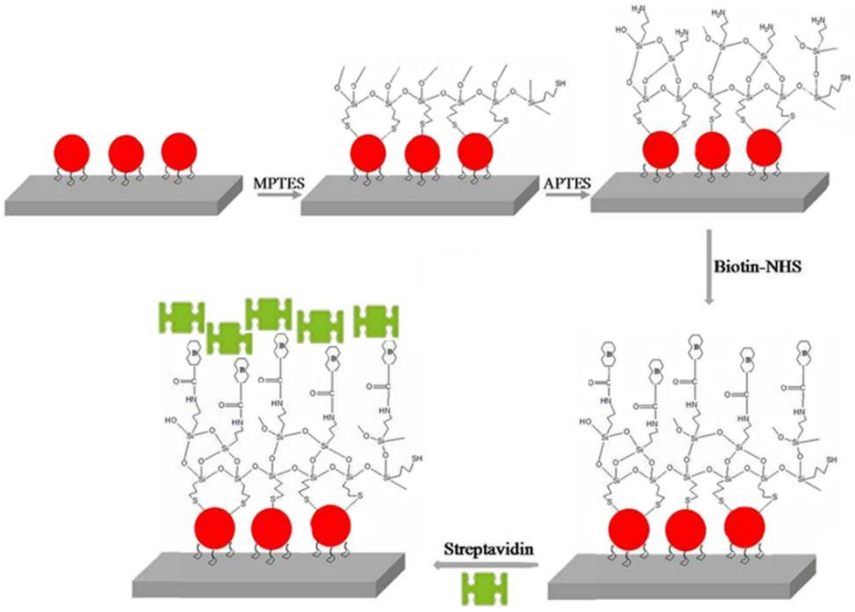

Scheme 1. Schematic illustration representing the functionalization steps involved in the fabrication of plasmonic platform for streptavidin detection.

For a better immobilization of biotin-NHS, the metallic surface of the annealed substrate was chemically modified with two self-assembled monolayers (SAM) (*i.e.* MPTES and APTES) deposited *via* the layer-by-layer method (Zhang, 2008). The first step of the label-free biosensing protocol consisted in functionalizing the annealed AuNSs substrate through immersion in a 1% MPTES methanol solution for 30 min, resulting in the formation of a silane-terminated MPTES SAM on the plasmonic surface. After carefully rinsed with methanol and water, the modified substrate was silanized in 4 % APTES ethanol solution for 20 min. After attaching the linkers, biotin-NHS was anchored onto the metallic surface of functionalized-AuNSs by immersing the substrate into 50 μg/mL biotin solution for 24 h. Afterwards, a large amount of phosphate buffered saline (PBS) solution was used to flush away the unreacted biotin-NHS from the metallic surface. Then, in order to eliminate the influence of nonspecific adsorption, the surface was then blocked with BSA

ACCEPTED MANUSCRIPT

by immersing the substrate in a solution of 50 μg/mL BSA in PBS for 1 h. After rinsing with water, the biotin-functionalized annealed AuNSs substrate was used as LSPR biosensor for the specific detection of streptavidin. To allow the capture of streptavidin, the biotin-functionalized substrate was incubated with streptavidin solution at 4 ^{o}C for 5 h. In order to determine the limit of detection of the proposed LSPR biosensor, different streptavidin concentrations (*i.e.* 5 nM, 10 nM, 20 nM, 35 nM and 50 nM in PBS, pH 7.4) were tested.

2.5. *Coupling of AuNRs with streptavidin in solution to enhance LSPR shifts for more detection sensitivity*

In order to enhance the detection sensitivity of the annealed AuNSs substrate, negatively charged streptavidin with concentrations ranging from 2 nM to 50 nM were directly attached to positively charged CTAB bilayer wrapped around AuNRs in aqueous solution (stock concentration 1.06×10^{-9} M, as calculated from the absorbance of longitudinal plasmon resonance for a molar extinction coefficient of $\varepsilon = 3.52 \times 10^{9}$ M^{-1} cm^{-1} (Orendorff and Murphy, 2006)) for 1 h. By dividing the concentration of streptavidin (2-50 nM) to the concentration of AuNRs in solution we find that the number of streptavidin molecules per AuNR roughly varies between 2 and 50. Extinction spectra were recorded before and after streptavidin adsorption onto the AuNRs's surface. Then, the biotin-functionalized substrate was incubated with streptavidin- labelled AuNRs at 4 ^{o}C for 5 h.

2.6. *Characterization methods*

The synthesized AuNSs and AuNRs in aqueous solution were firstly characterized by measuring their UV-Vis-NIR absorption spectra at room temperature using a Jasco V-670 spectrophotometer with a band width of 2 nm and 1 nm spectral resolution. Optical extinction measurements on plasmonic substrates before and after annealing were taken with a Zeiss Axio Observer Z1 inverted microscope (20× objective, LD Plan-Neofluar, NA = 0.4, Zeiss) with transmitted broadband light coupled into a portable Ocean Optics USB4000 microspectrometer controlled by Spectra Suite software.

The morphology of the plasmonic substrates before and after thermal annealing process was investigated in air at room temperature by transmission electron microscopy (TEM) using a JEOL JEM 1010

Accepted manuscript

ACCEPTED MANUSCRIPT

transmission electron microscope and by tapping mode atomic force microscopy (AFM) using a WITec alpha 300A microscope and aluminium coated tip. The AFM image was recorded on an area of 2 μm × 2 μm, 256 × 256 pixels at a moving speed of 1s per line.

The Raman and SERS spectra were acquired with a Confocal Raman Microscope (alpha 300R from WITec GmbH, Ulm, Germany) employing for excitation the 632.8 nm light from a He-Ne laser. The SERS signals were collected through a confocal pinhole of 100 μm by using a 0.9 NA objective of 100× magnification. The reference Raman spectra of Biotin-NHS were recorded through a 20× objective (NA = 0.4). The measurements were conducted at a laser power incident on the sample of 3 mW, and the integration time was set at 3 s per spectrum.

3. Results and Discussion

3.1 Optical and morphological characterization of the fabricated LSPR biosensor.

Typical UV-Vis-NIR extinction spectra of the self-assembled AuNSs on the functionalized glass substrate before and after thermal annealing process are presented in Fig. 1A. Before annealing, the plasmonic substrate displays a broad plasmonic band in NIR region at 710 nm with a shoulder at 535 nm. In particular, the shoulder at 535 nm is associated to the plasmon resonance of isolated AuNSs while the NIR band is assigned to the partial aggregated (due to existing assemblies) AuNSs formed on the functionalized substrate, in good agreement with AFM and TEM imaging observations (Fig. 1B and 1E). Furthermore, it can be clearly observed from AFM and TEM images that most of the AuNSs are self-assembled in small clusters and only a few isolated AuNSs can be found on the substrate. To note that from the recorded AFM cross-section, the height of these isolated AuNSs is around 16-20 nm (Fig. 1D - black spectrum), similar to the value obtained for colloidal AuNSs (Suarasan et al., 2013), thus showing that the AuNSs preserve their size. Interestingly, the thermal annealing at 500 °C for 90 min leads to dramatic changes in the extinction spectrum of the self-assembled AuNSs. Specifically, the broad asymmetric peak from NIR region assigned to the coupled AuNSs – band which reflects the local density of the AuNSs as well as the degree of their assembling as we previously reported (Toderas et al., 2007) – completely disappears due to the coalescence effect of initial AuNSs into newly formed individual larger AuNSs with a well-defined single LSPR response at around 536 nm. The morphological changes of the substrate induced by the thermal annealing treatment

Accepted manuscript

ACCEPTED MANUSCRIPT

(Fig. 1C and 1F) confirm the LSPR response. Specifically, at this high temperature the height of the new formed AuNSs is around 50-60 nm (Fig. 1D - red spectrum). Furthermore, according to the TEM image analysis produced by using an image processing Image J toolkit (ImageJ), the average number of AuNSs decreases from 1578 (Fig. 1E) to 259 per TEM area (Fig. 1F) and the distance between them becomes almost twice larger than their diameters. However, it should be noted that the annealed AuNSs substrates are stable, as the plasmonic response was almost constant after 1 month.

We assume that the formation of higher AuNSs could possible arise from two mechanisms operating concurrently: i) coalescence of AuNSs – process most common for a high density of clusters, involving the merging of small AuNSs into larger AuNS and ii) Ostwald ripening process which occurs by the removal of atoms from one AuNSs *via* substrate surface diffusion and transfer to another one (Bechelany et al., 2010; Wang et al., 2009).

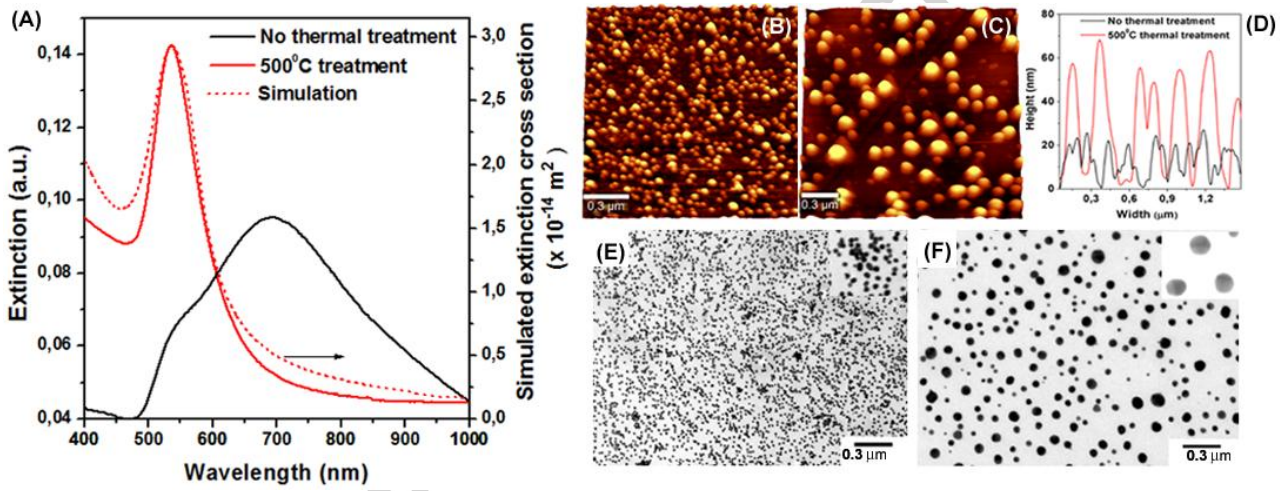

Fig. 1. (A) Extinction spectra of the AuNSs assemblies before (black spectrum) and after annealing (red spectrum) and FDTD simulated extinction cross section (red dotted spectrum) of the substrate after annealing; AFM and TEM images of the AuNSs self-assembled on glass surface before (B and E) and after (C and F) thermal annealing; (D) Cross-sections before (black spectrum) and after (red spectrum) thermal annealing.

In order to get a better insight into the experimental optical response of the thermally treated substrate, we conducted numerical simulation by employing the Finite-Difference Time-Domain (FDTD) method using the commercially available FDTD Solutions software from Lumerical Inc (FDTD Solutions |

ACCEPTED MANUSCRIPT

Lumerical's Nanophotonic FDTD Simulation Software) as described in SI. The simulated extinction cross section (Fig. 1A – red dotted spectrum), obtained for the morphology considered in simulation (Fig. S2A), mimics rather well the experimental results.

To assess the biosensing capability of the annealed plasmonic substrate, we also simulated the sensitivity of the designed substrate to the change of the local refractive index (RI). In general, the bulk refractive index sensitivity (S) of a plasmonic nanostructure is dependent on its size, shape and material composition (Miller and Lazarides, 2006) and is defined as the wavelength shift of the LSPR peak in response to the change of the refractive index of the surrounding environment (in nm / refractive index unit (RIU)). In our case, S was theoretically determined from the plot in Fig. S2B, showing the dependence of the LSPR band position against the RI of the surrounding media for the indicated values. After performing a linear regression, the slope of the fitted line indicated a sensitivity of 81 nm/RIU for our substrate.

3.2. Biosensing capability of plasmonic substrate

The LSPR spectra corresponding to different biofunctionalization steps involved in the fabrication of plasmonic platform for streptavidin detection are presented in Fig. 2A. As previously showed, the annealed self-assembled AuNSs substrate exhibits a well-defined LSPR band at 536 nm. After incubation with biotin, the plasmonic extinction peak of the substrate red-shifts 3 nm, indicating the success biofunctionalization (Fig. 2A – spectrum b). Such spectral modifications are commonly observed in the case of LSPR biosensors and can be assigned to the increase of the local refractive index, transduced by plasmonic tuning of the resonance band – including here resonant wavelength shift or/and maximum optical density changes (Jia et al., 2014). However, in our case, following the APTES modification, an amino-containing SAM is formed, which facilitates the chemical binding to biotin-NHS *via* an amination reaction (Niu et al., 2013). The covalent bonds of biomolecules to Au surfaces are – in general – preferred over electrostatic or adsorption interaction which might lead to the desorption of biomolecules. Subsequently, when streptavidin target molecules are immobilized onto the biotin-functionalized plasmonic substrate (Fig 2A - spectrum c and inset), a large red-shift of 10 nm is recorded, which is attributed to the change of the local refractive index generated by the specific detection of streptavidin.

Accepted manuscript

ACCEPTED MANUSCRIPT

The LSPR response of the plasmonic biosensor as a function of streptavidin concentration (from 5 to 50 nM) is presented in Fig. 2B. The LSPR maximum is shifted to longer wavelengths upon streptavidin binding, with the magnitude of the red-shift increasing from 1 to 10 nm with streptavidin concentration. To note that the LSPR response gets saturated for a concentration higher than 35 nM.

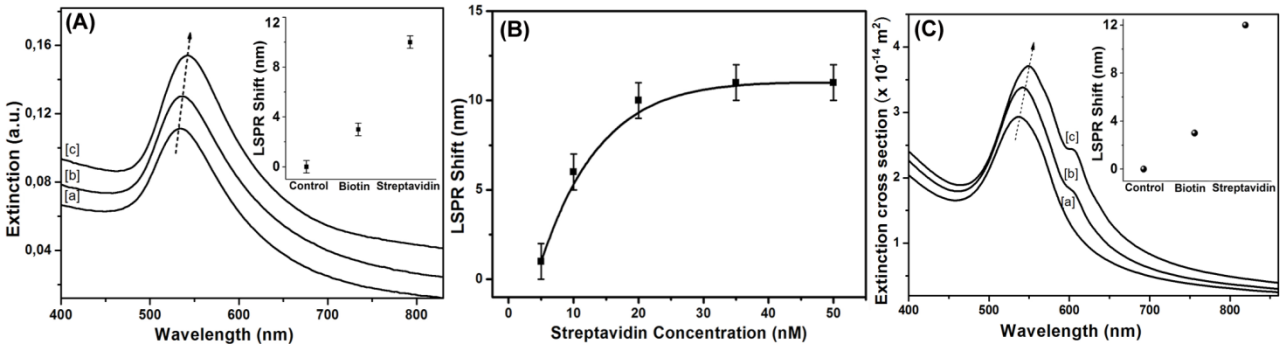

Fig. 2. (A) Extinction spectra of annealed AuNSs platform before (a) and after incubation with biotin-NHS (b) and streptavidin (50 nM) (c) solutions. The inset shows the LSPR peak shift after biotin-streptavidin binding; (B) LSPR response of the plasmonic platform as a function of streptavidin concentration. The error bars represent the standard deviation resulted from three independent measurements. (C) FDTD simulated extinction cross section obtained for the considered morphology before (spectrum a) and after coating with biotin (spectrum b) and streptavidin (spectrum c). The inset shows the simulated LSPR peak shift after biotin-streptavidin binding.

The simulated optical response of our substrate after the binding of biotin and streptavidin was also simulated, as explained in SI. The simulated extinction cross section presented in Fig. 2C shows LSPR shifts of 3 nm and 12 nm after interaction with biotin (spectrum b) and streptavidin (spectrum c), respectively, in good agreement with experimental results.

3.3. SERS detection of streptavidin using the biotin-functionalized AuNSs substrate

SERS is a highly specific and sensitive analytical technique useful for investigating molecular composition in a non-destructive manner as it enables an ultrasensitive detection, down to a single molecule (Abbas et al., 2013; Santos et al., 2009), and provides structural information about the molecular species

ACCEPTED MANUSCRIPT

from their unique vibrational Raman fingerprint (Aroca, 2006; Baia et al., 2008). The SERS phenomenon relies on the collective oscillation of the conduction electrons emerging at the surface of noble-metal nanostructures under light excitation, known as surface plasmons (SP), which enhance significantly the optical near fields. As a consequence, the Raman scattering from molecules located in close proximity is significantly enhanced, with up to 8-10 orders of magnitude, by the so-called electromagnetic effect (EM), the mechanism accepted as being mainly responsible for the SERS effect. In particular, when an analyte is adsorbed onto so-called "hot-spots", such as gaps and junctions created between interconnected nanoparticles, its Raman signal can be considerably enhanced, which allows detection up to single-molecule (Aroca, 2006; Baia et al., 2008). For that reason, beyond LSPR spectroscopy, the capture and adsorption of streptavidin onto the surface of biotin-functionalized AuNSs platform was also proved by SERS analysis. Comparative SERS measurements were performed on biotin-AuNSs platform before and after the adsorption of streptavidin. Fig. 3A- spectrum b shows a representative SERS spectrum collected from biotin-AuNSs substrate. For comparison, the Raman spectrum of solid biotin is also shown in Fig. 3A- spectrum a. The presence of the same spectral features in both Raman and SERS spectra clearly proves the adsorption of biotin molecules onto the surface of AuNSs substrate. The assignment of the major vibrational bands is given in Fig. 3B.

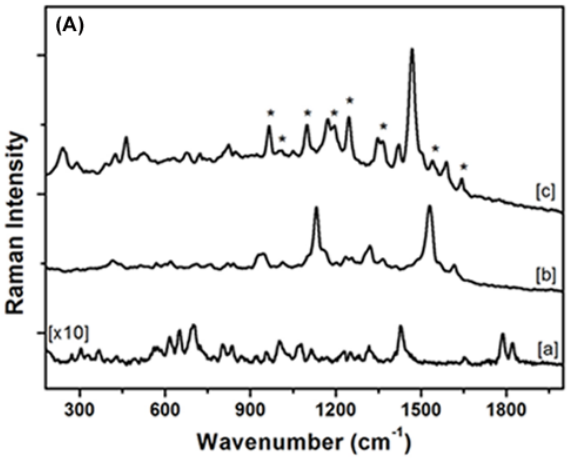

(B)

SERS biotin (cm^{-1})	SERS biotin/streptavidin complex (cm^{-1})	Assignment (Bi et al., 2013; Galarreta et al., 2011; Wang and Schultz, 2013)
932	-	Trp(W25), Glu, Asp
948	965	Trp, Val
1010	1010	Trp(W16), Phe, Ala
-	1097	Glu, Thr
1131	-	C-N stretching, Trp(W13), Val, Glu
1163	1172	Phe, Tyr, Val
1203	1200	Tyr 7a
1239	1244	amide III (r. coil)
1317	-	Ser (CH_2 bending)
-	1348	Trp(W7)
1364	1364	Trp(W7)
-	1468	CH_2 ring stretching
1530	1535	amide II vibration due to N–H bending and C-H stretching
1615	-	C-C wagging
1653	1642	amide I vibration due to C=O stretching

Fig. 3. (A) Normal Raman spectrum of solid biotin-NHS multipled by 10 (a), SERS spectra of biotin-functionalized AuNSs platform (b) and streptavidin adsorbed onto the biotin-functionalized AuNSs platform (c); (B) Assignment of the major SERS bands in the spectra of biotin and biotin/streptavidin complex illustrated in A.

For example, the prominent band at 1131 cm^{-1} observed in the SERS spectrum corresponds to the Trp13, C-N stretching vibrations (Bi et al., 2013). The vibrational bands at 1615, 1530 and 1364 cm^{-1} are assigned to C-C wagging, amide II vibration due to N-H bending and C-H stretching and Trp 7, respectively, according to the literature (Bi et al., 2013; Galarreta et al., 2011). A dramatic change of SERS fingerprint is observed after the adsorption of streptavidin molecules. As shown in Fig. 3A- spectrum c and Fig. 3B, the vibrational bands of biotin (marked by *) are present in the spectrum together with the characteristic bands of streptavidin molecules. In particular, the bands at 1642, 1468, 1244, 1097 and 965 cm^{-1} are assigned to amide I vibration due to C=O stretching, CH_2 ring bending, amide III (r. coil), Glu, Thr and Trp, Val vibrations of streptavidin, respectively.

The reproducibly of the SERS signal is an important requirement for any analytical applicability of a SERS platform. The SERS reproducibility of the fabricated biotin-AuNSs platform was tested by recording several SERS spectra from random multiple sites on the substrate surface. As shown in Fig. S3 we only noticed a difference between the overall intensities with no significant change of the band positions, full widths of bands and peak/peak intensity ratios.

3.4. Enhancing the LSPR shift

In order to enhance the LSPR sensor reponse, we propose a new strategy using AuNRs as amplification labels. Specifically, we performed the same experiments replacing the free streptavidin (hereafter, SA) with streptavidin-conjugated AuNRs (hereafter, AuNRs@SA). Experimentaly, 2, 5, 20 and 50 nM streptavidin solutions were incubated with AuNRs in aqueous solution for 5 h to allow the conjugation to occur *via* electrostatic binding (Zhou et al., 2012). The synthesized AuNRs exhibit in solution a weak transverse LSPR band at 511 nm and a strong longitudinal LSPR band at 717 nm (Fig. 4A - red spectrum). Following incubation with streptavidin at high concentration (*i.e.* 20 and 50 nM), the longitudinal LSPR band is broadened and its intensity is significantly reduced (Fig. 4A). This change of the LSPR response was attributed to the plasmon coupling effect, which is typically induced by AuNRs aggregation (Vial et al., 2007). Interestingly, when AuNRs were incubated with lower streptavidin concentrations (*i.e.* 2

Accepted manuscript

ACCEPTED MANUSCRIPT

and 5 nM), only a red shift of 7 nm and 14 nm, respectively, in the longitudinal LSPR peak was recorded together with the slight decrease of the intensity band (Fig. 4A - blue and green spectra). It is worth mentioning that the concentration of 2 nM was the lowest concentration at which an LSPR shift was distinguished.

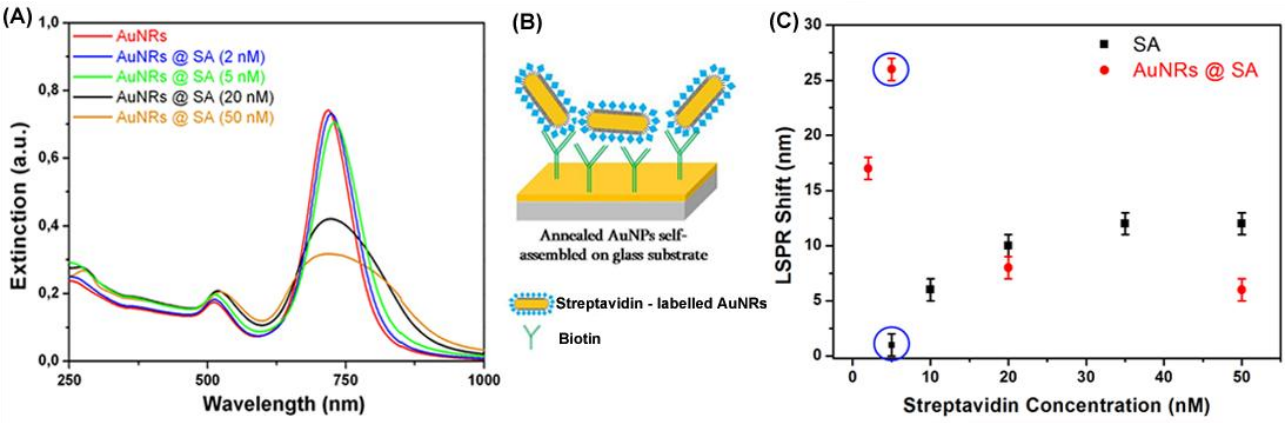

Fig. 4. (A) Conjugation of AuNRs in aqueous solution with streptavidin at different concentrations; (B) Schematic representation of using streptavidin labelled-AuNRs to increase the LSPR biosensor response; (C) Quantitative LSPR sensor response for free streptavidin (here, SA) and streptavidin labeled-AuNRs (here, AuNRs@SA).

Similar to previous experiment of LSPR detection using free streptavidin, the plasmonic substrate was functionalized with biotin-NHS and subsequently exposed to the different batches of as-prepared AuNRs@SA. Interestingly, using this detection scheme, the extinction spectrum of the plasmonic substrate shifts 26 nm toward longer wavelengths after the coupling of AuNRs@SA (5 nM) contrary to the solely 1 nm wavelength shift obtained in the absence of AuNRs (Fig. S4). In this context, a 26- fold enhancement of the LSPR response was recorded for 5 nM streptavidin concentration (Fig. 4C, marked points in the plot). Furthermore, it is important to note here that we achieved to detect a streptavidin concentration of 2 nM using the proposed sensing amplification strategy, as the LSPR band still shifts 17 nm, proving thus the ability of this strategy to enhance LSPR shifts for more sensitive detection of low concentrations of streptavidin. Contrarily, following incubation with streptavidin labeled-AuNRs at high concentration (herein 20 and 50 nM streptavidin) we were not able to detect a LSPR shift response as high as obtained for a lower

ACCEPTED MANUSCRIPT

streptavidin concentration, most probably due to the aggregated streptavidin-labeled AuNRs systems (Fig. 4C). Therefore, we assume that this sensing amplification strategy could be employed only for individual streptavidin-metallic NPs hybrid systems.

In order to obtain a better understanding on the LSPR shift enhancement obtained in presence of AuNRs, we simulated the simple case of an individual AuNS of 60 nm diameter coated with biotin and investigated whether coupling with AuNRs will induce a supplementary LSPR shift. Specifically, we compared the LSPR shift of the considered biotin-coated AuNS after coating with streptavidin with the shift obtained after coupling biotin-coated AuNS with a set of streptavidin-labeled AuNRs (see SI for detailed description). Considering the shift of the longitudinal LSPR, we can assume that streptavidin molecules are bounded preferentially at the ends of AuNRs, inferring thus that the streptavidin-labeled AuNRs would assume a tilled orientation onto the substrate allowing their both streptavidin- labeled ends to interact with the immobilized biotin. Therefore we considered in our simulation that AuNRs are located at 3.8 nm from the gold surface that is the thickness of biotin layer. Also, we considered a single excitation source, oriented transversal to the longitudinal axe of AuNRs, to support better the plasmonic coupling between the two types of plamonic nanostructures. However, we cannot exclude that experimentally, AuNRs assume various orientation on the immobilized AuNSs which implied that the plasmonic coupling and subsequently, the optical response, would approach the case of unpolarized light source.

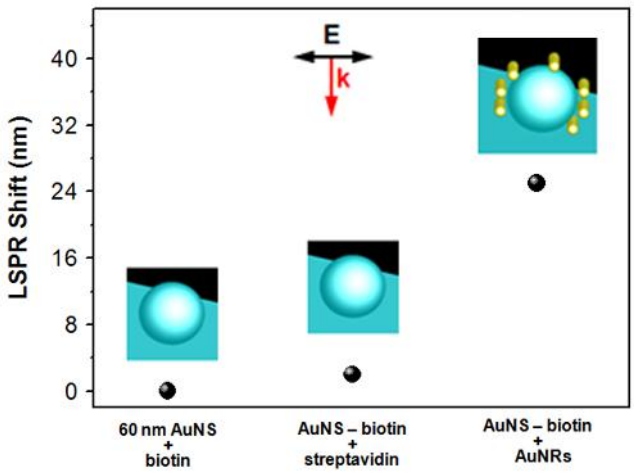

Fig. 5. Simulated LSPR shift obtained for 60 nm AuNS covered by biotin, conjugated with streptavidin and AuNRs.

ACCEPTED MANUSCRIPT

As shown in Fig. 5 the LSPR band of biotin-covered 60 nm AuNS shifts by 2 nm after coating with streptavidin. Interestingly, the shift is enhanced to as high as 25 nm after coupling with streptavidin-labeled AuNRs, in the configuration described above and depicted in the plot, confirming our experimental results regarding the enhancement of LSPR sensitivity.

Thus, we believe that the enhancement of the detection sensitivity of our designed LSPR sensor is probably due to a combination of two mechanisms*: i)* the AuNRs increases the refractive index change following streptavidin binding and *ii)* an effective plasmonic coupling between the streptavidin labeled-AuNRs and annealed plasmonic substrate. Van Duyne *et al* demonstrated that antibody-labeled spherical AuNPs could increase the observed LSPR shift by up to 400 % as compared to similar concentrations of free antibody (Hall et al., 2011b). We believe that AuNRs are preferable to AuNSs due to their large plasmonic tunability from the visible to NIR spectral range (Marinakos et al., 2007), an important property that allows to further optimize the sensitivity enhancement *via* an effective plasmonic coupling between anisotropic NPs and plasmonic substrate.

4. Conclusion

In this work, we developed an efficient plasmonic biosensor based on annealed spherical gold nanoparticles (AuNSs) self-assembled on solid surface for the detection of specific biotin-streptavidin interaction. It was found that the substrate treated at high temperature (here 500 °C) has a sharper well-defined LSPR response in the visible spectrum range. The as-designed biosensor was successfully implemented as LSPR biosensor for the detection of streptavidin in buffer solution. For this purpose, the capture biotin molecules were immobilized on annealed plasmonic substrate and then incubated with increasing concentrations of streptavidin, achieving a limit of detection (LOD) of 5 nM. In addition, we demonstrate the feasibility of this platform/biosensor to detect and identify streptavidin through Surface Enhanced Raman Scattering (SERS), a molecular identification technique that offers qualitative information about the assay. Interestingly, the response from LSPR biosensor was 26-fold improved when using a simple strategy based on streptavidin-labeled AuNRs onto a biotin-functionalized LSPR sensor compared to the free streptavidin assay. More importantly, by using AuNRs as amplification labels we achieve a LOD of

Accepted manuscript

ACCEPTED MANUSCRIPT

streptavidin of 2 nM. Moreover, our experimental results were confirmed by the performed numerical simulations. The development of such efficient LSPR/SERS platforms with unique capabilities -that could be further simply integrated within microfluidic device- becomes highly promising for future point-of-care diagnostic assays.

Acknowledgments. This work was supported by CNCS - UEFISCDI Romania, under the project number PN-II-PT-PCCA-2013-4-1961.

References

Abbas, A., Tian, L., Morrissey, J.J., Kharasch, E.D., Singamaneni, S., 2013. Adv. Funct. Mater. 23, 1789–1797.

Al Balushi, A.A., Zehtabi-Oskuie, A., Gordon, R., 2013. Biomed. Opt. Express 4, 1504–1511.

Ament, I., Prasad, J., Henkel, A., Schmachtel, S., Sönnichsen, C., 2012. Nano Lett. 12, 1092–1095.

Anker, J.N., Hall, W.P., Lyandres, O., Shah, N.C., Zhao, J., Van Duyne, R.P., 2008. Nat. Mater. 7, 442–453.

Aroca, R., 2006. Surface-Enhanced Vibrational Spectroscopy. John Wiley & Sons, Chichester.

Baia, M., Astilean, S., Iliescu, T., 2008. Raman and SERS Investigations of Pharmaceuticals. Springer-Verlag GmbH, Berlin, Heidelberg.

Bechelany, M., Maeder, X., Riesterer, J., Hankache, J., Lerose, D., Christiansen, S., Michler, J., Philippe, L., 2010. Cryst. Growth Des. 10, 587–596.

Bi, L., Dong, J., Xie, W., Lu, W., Tong, W., Tao, L., Qian, W., 2013. Anal. Chim. Acta 805, 95–100.

Canpean, V., Gabudean, A.M., Astilean, S., 2013. Colloids Surf. Physicochem. Eng. Asp. 433, 9–13.

FDTD Solutions | Lumerical's Nanophotonic FDTD Simulation Software, URL https://www.lumerical.com/tcad-products/fdtd/

Galarreta, B.C., Norton, P.R., Lagugné-Labarthet, F., 2011. Langmuir 27, 1494–1498.

Geng, Z., Kan, Q., Yuan, J., Chen, H., 2014. Sens. Actuators B Chem. 195, 682–691.

Guo, L., Jackman, J.A., Yang, H.-H., Chen, P., Cho, N.-J., Kim, D.-H., 2015. Nano Today 10, 213–239.

Guo, L., Kim, D.-H., 2012. Biosens. Bioelectron. 31, 567–570.

Accepted manuscript

ACCEPTED MANUSCRIPT

Hall, W.P., Modica, J., Anker, J., Lin, Y., Mrksich, M., Van Duyne, R.P., 2011a. Nano Lett. 11, 1098–1105.

Hall, W.P., Ngatia, S.N., Van Duyne, R.P., 2011b. J. Phys. Chem. C 115, 1410–1414.

ImageJ, URL http://rsb.info.nih.gov/ij/

Jia, K., Khaywah, M.Y., Li, Y., Bijeon, J.L., Adam, P.M., Déturche, R., Guelorget, B., François, M., Louarn, G., Ionescu, R.E., 2014. ACS Appl. Mater. Interfaces 6, 219–227.

Liley, M., Keller, T.A., Duschl, C., Vogel, H., 1997. Langmuir 13, 4190–4192.

Marinakos, S.M., Chen, S., Chilkoti, A., 2007. Anal. Chem. 79, 5278–5283.

Mayer, K.M., Hafner, J.H., 2011. Chem. Rev. 111, 3828–3857.

Miller, M.M., Lazarides, A.A., 2006. J. Opt. Pure Appl. Opt. 8, S239–S249.

Nikoobakht, B., El-Sayed, M.A., 2003. Chem. Mater. 15, 1957–1962.

Niu, L., Cheng, K., Wu, Y., Wang, T., Shi, Q., Liu, D., Du, Z., 2013. Biosens. Bioelectron. 50, 137–142.

Orendorff, C.J., Murphy, C.J., 2006. J. Phys. Chem. B 110, 3990–3994.

Rich, R.L., Myszka, D.G., 2010. J. Mol. Recognit. JMR 23, 1–64.

Santos, D.P. dos, Andrade, G.F.S., Temperini, M.L.A., Brolo, A.G., 2009. J. Phys. Chem. C 113, 17737–17744.

Suarasan, S., Focsan, M., Maniu, D., Astilean, S., 2013. Colloids Surf. B Biointerfaces 103, 475–481.

Svedendahl, M., Chen, S., Dmitriev, A., Käll, M., 2009. Nano Lett. 9, 4428–4433.

Szunerits, S., Boukherroub, R., 2012. Chem. Commun. 48, 8999–9010.

Toderas, F., Baia, M., Baia, L., Astilean, S., 2007. Nanotechnology 18, 255702.

Turkevich, J., Stevenson, P.C., Hillier, J., 1951. Discuss. Faraday Soc. 11, 55–75.

Vial, S., Pastoriza-Santos, I., Pérez-Juste, J., Liz-Marzán, L.M., 2007. Langmuir 23, 4606–4611.

Voue, M., Goormaghtigh, E., Homble, F., Marchand-Brynaert, J., Conti, J., Devouge, S., De Coninck, J., 2007. Langmuir 23, 949–955.

Wang, Y.Q., Liang, W.S., Geng, C.Y., 2009. Nanoscale Res. Lett. 4, 684–688.

White, I.M., Fan, X., 2008. Opt. Express 16, 1020.

Zhang, S., 2008. Surface plasmon resonance and its applications to the probing of macromolecules on gold surfaces. East China Normal University, Shanghai, China.

Accepted manuscript

ACCEPTED MANUSCRIPT

Zhao, J., Zhang, X., Yonzon, C.R., Haes, A.J., Van Duyne, R.P., 2006. Nanomed. 1, 219–228.

Zhou, X., Wang, Y., Zhong, L., Bao, S., Han, Y., Ren, L., Zhang, Q., 2012. Nanoscale 4, 6256–6259.

Highlights

- A simple and efficient strategy to improve the sensitivity of LSPR shift-based biosensors was proposed.
- Biotin-streptavidin recognition interaction was used as proof-of-concept for the detection assay.
- By employing gold nanorods as amplification labels, the sensitivity of the LSPR nanosensor was 26-fold enhanced.
- Such plasmonic nanosensors could become highly promising for future point-of-care diagnostic assays.

Accepted manuscript